https://doi.org/10.2352/ISSN.2169-2629.2017.32.136

Improvement of Appearance from Motion by using Omni-Directional Camera

Ryota Domon1), Shoji Yamamoto2), Hiroshi Kintou3), Norimichi Tsumura1)
1) Graduate School of Advanced Integration Science, Chiba University, CHIBA, JAPAN
2) Tokyo Metropolitan College of Industrial Technology, TOKYO, JAPAN
3) Nikon Corporation, TOKYO, JAPAN

Abstract

We present a rapid measurement method for material appearance based on surface reflectance properties of three-dimensional object. Conventional methods have some problems relating to the size, cost, and difficulty of operation. Appearance from Motion method proposed by Dong et al. is appropriate to conquer above problem. Their method challenged to estimate the surface reflectance under unknown lighting. However, a use of multiple unknown parameters causes the loss of convergence, and sometimes preys on the accuracy and computational cost. Therefore, we improved the algorithm of Appearance from Motion method to use the omni-directional camera for incident lighting component. We demonstrate valuable results for accuracy of reproduction and reduction of computational cost by using the omni-directional camera.

Introduction

The important information of surface reflectance is useful for the field of computer graphics. This information is defined as bi-directional reflectance distribution function (BRDF) to calculate an appearance of object. Various profile of BRDF change the material appearance based on dichromatic reflection model. Especially, specular reflection represents the surface smoothness by its degree of reflection.

Conventionally, the use of BRDF information was limited in the field of computer graphics. Recent revolution of three-dimensional (3D) printing technology gives us the useful chance of BRDF information in real production. Actually, there are many applications of using three-dimensional printing, reproducing in industrial products, arts, and regenerative medicine. The most expected contribution of 3D printer is application for rapid proto-typing that is compatible to final product with same property of surface roughness. Therefore, the method of BRDF measurement attracts attention as the essential tool for advancement of 3D printing technology.

Various measurement methods have been proposed for the accurate BRDF of real object. However, the currently used method or instruments are large scale and need high calculation cost. Moreover, it is difficult for non-expert user to measure the appearance of the object. The rapid reproduction is also important characteristics of 3D printings. For this reasons, the measurement system, which is commercially available, rapid and compact, is required for handling the appearance.

In this paper, therefore, we propose a rapid and compact measurement system that is expected to be equipped with 3D printing system. Our method refers to Appearance from Motion method proposed by Dong et al. [1]. We improve their method by using an omni-directional camera for incident lighting component. This reformation provides the accuracy and simplification compared with previous method. Even now, a part of this research has presented as a concept of our research in JSAP 2016, Niigata [2]. This paper describes a detail algorithm and result of demonstration by using our proposed method.

Related Works

Appearance reproduction is well-studied with BRDF, which is physical model for representing photon propagation. There are many kinds of appearance measurement method or instruments [3]-[18]. Gonio-photometer and many prior works can be referred to acquiring the BRDF parameters for reproduction of various appearances. Unfortunately, accurate BRDF measurement needs 6 DOF movement and precious position arrangement. Therefore, large scaled equipment and long measurement time are required. Our method is stimulated by “Appearance from Motion” proposed by Dong et al. [1], which acquires the reflectance at spatially varying isotropic surface under unknown lighting. Because acquisition scheme of this method is greatly simplified, only capturing the video while rotating the objects, non-expert users are also accessible and easy to control. In this appearance from motion system, they estimated three unknown variables; distribution of specular highlights, reflectance, and lighting condition, under the condition that the shape of object is known. Dong et al. attempted to set various restrictions to solve this complex problem and demonstrated feasible result of acquiring the surface reflectance.

However, the estimation of three variables causes less convergence and more computational cost. The reflectance property is very important because it would be the most significant factor of appearance. On the other hand, the lighting component will have an insignificant importance because lighting condition is easy to measure by using omni-directional cameras that become compact and low price. Therefore, we improve and simplify the Dong’s method for the guarantee of convergence and rapid estimation under known lighting condition, which is derived environmental image captured by omni-directional cameras.

Method

Acquisition & Calibration

Our proposed method requires the measured images of object that is rotating on the table, environmental image to provide an incident lights on the target object, and geometry data of target object. We captured images of object on the rotating table by digital camera (Nikon D5100) equipped with varifocal lens (AF-S NIKKOR 24-120mm). These images were saved by single exposure radiometrically linear RAW images, and intrinsic camera parameters were precomputed by using the method of Zhang et al. [19]. Environmental image was also captured by omni-directional camera (Ricoh Theta). In order to use this image captured with omni-directional camera as the incident light component, it is necessary to consider the radiometrically linearity and color matching with digital camera. To solve this problem, we reproduced high dynamic range (HDR) image by capturing 11 images with different exposure values. HDR composition was carried out with the method proposed by Debevec et al. [20]. Moreover, we used Munsell color chart for linear correction and performed the color matching between digital camera and omni-directional camera. Through these processing, we derived incident light component from omni-directional camera as shown in Fig.1. The object is rotated by a rotational stage (SGSP-60YAW, Sigma-Koki). We modeled each target objects by hand, such as simple plate or cylinder. We register the geometry manually for the first frame of image sequences. Subsequent frames are automatically registered since the center of rotation is consistent.

Figure 1
Tone-mapped HDR image captured by omni-directional camera

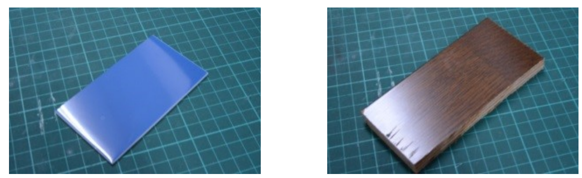

(a) Ceramic plate (b) Wooden Flooring plate

Figure 2
Various spatial distribution of highlights in real world material

Assumptions and input data

Our proposed method refers to the pioneering idea proposed by Dong et al. [1]. We assume that surface reflectance is isotropic and it is expressed by microfacet reflectance model. As the dichromatic BRDF model is used in our system, the surface reflectance at a point x is defined by Eq.1,

$$f(\boldsymbol{\omega}_\mathbf{i},\boldsymbol{\omega}_o;x)=\frac{\rho_d(x)}{\pi}+\rho_s(x)f_s(\boldsymbol{\omega}_\mathbf{i},\boldsymbol{\omega}_o;x) \quad , \quad (1)$$

where $\boldsymbol{\omega}_\mathbf{i}$ and $\boldsymbol{\omega}_\mathbf{o}$ are the incident and reflected directions, ρ_d and ρ_s are the diffuse and specular reflectance, and f_s is the specular reflectance function, which is proposed by Asikhmin et al. as follows [21] .

$$f_s(\boldsymbol{\omega}_\mathbf{i},\boldsymbol{\omega}_o)=\frac{D(\boldsymbol{\omega}_\mathbf{h})G(\boldsymbol{\omega}_\mathbf{i},\boldsymbol{\omega}_o)F(\boldsymbol{\omega}_\mathbf{i},\boldsymbol{\omega}_o)}{4(\mathbf{i}\cdot\mathbf{n})(\mathbf{o}\cdot\mathbf{n})} \quad , \quad (2)$$

where $D(\boldsymbol{\omega}_\mathbf{h})$ indicates the microfacet normal distribution function (NDF) of the halfway direction $\boldsymbol{\omega}_\mathbf{h}$, $F(\boldsymbol{\omega}_\mathbf{i},\boldsymbol{\omega}_o)$ indicates Fresnel reflectance function (we assumed a fixed index of refraction of 1.3 for all materials as same as Dong et al.) , and $G(\boldsymbol{\omega}_\mathbf{i},\boldsymbol{\omega}_o)$ indicates the shadowing and masking function. Because specular highlights are quite effective factor for appearance reproduction, it is very important to select the spatial distribution of specular highlights, namely NDF. We observed two major trends of spatial distribution of highlights in real world. Ceramic plates have weak tail in highlights as shown in Fig.2 (a). On the other hands, wooden flooring plate has relatively strong tail in highlights as shown in Fig.2 (b). Therefore, we employed two NDFs owing to represent these characteristics. First, we adopt Beckmann distribution model to express the weak tail in highlight as shown in Fig.2 (a). In other case, GGX model is adopted to express the strong tail in highlight as shown in Fig.2 (b). These models determine the spatial distribution by the angles between halfway direction ω_h and surface normal. For the simplification of acquiring the surface reflectance properties, we seek the roughness parameters of each model as the objective function instead of the 1-dimensional tabulated function that monotonically decreased used in previous study.

By solving the minimization problem, it is possible to obtain an appropriate value (surface reflectance properties) with residual simultaneously. It can be regarded as the smaller residual is suitable for representing the surface reflectance properties. For the reduction of computational cost, we employed Smith's shadowing and masking term, which has relatively less computation cost.

In our method, three variables for each surface point are determined separately. To derive these parameters, we solve minimization problem denoted by Eq.3,

$$\underset{(\rho_d,\rho_s,D)_x}{\arg\min}\sum_t\sum_x \| I(\boldsymbol{\omega}'_o,x,t)-L(\boldsymbol{\omega}'_o,x,t)\|^2 \quad , \quad (3)$$

where $I(\boldsymbol{\omega}'_o,x,t)$ is the observation value of rotating target object, $L(\boldsymbol{\omega}'_o,x,t)$ is the outgoing radiance at a surface point x at time t. $\boldsymbol{\omega}'_o$ indicates the outgoing (viewpoint) vector, and prime symbol is the direction in global coordinate. $L(\boldsymbol{\omega}'_o,x,t)$ is determined by registered object geometry $\mathbf{n}(x,t)$ and incident light component $E(\boldsymbol{\omega}'_i)$ captured with omni-directional camera as denoted in Eq.4.

$$L(\boldsymbol{\omega}'_o, x, t) = \int_\Omega f_r(\boldsymbol{\omega}_i(x,t), \boldsymbol{\omega}_o(x,t); x) E(\boldsymbol{\omega}'_i)(\mathbf{n}(x,t)\cdot\boldsymbol{\omega}'_i) d\boldsymbol{\omega}'_i \quad , \quad (4)$$

where $\boldsymbol{\omega}_i$ and $\mathbf{n}$ indicates the lighting vector and surface normal at the surface point x. $\boldsymbol{\omega}_i$ is the sampling area from environmental map captured by omni-directional camera. We set the range of sampling area less than 0.5π from the mirror reflection with respect to the viewpoint vector in order to reduce the computational cost.

NDF Recovery

Our proposed method solves Eq.3 with each surface point separately. Thus, we rewrite Eq.3 to denote the equation of a single surface point x,

$$\underset{(\rho_d,\rho_s,D)_x}{\arg\min} \sum_t \| T(\boldsymbol{\omega}'_o, t) - L(\boldsymbol{\omega}'_o, t) \|^2 \quad , \quad (5)$$

where $T(\boldsymbol{\omega}'_o, t)$ is equal to $I(\boldsymbol{\omega}'_o, x, t)$, which represents the temporal variation at the surface point x as shown in Fig.3. It is difficult to solve Eq.5 because there are still three variables. Therefore, we take temporal gradient of observation and outgoing radiance on the surface point x. Temporal gradient of the outgoing radiance can be expressed as Eq.6.

$$\begin{aligned}
\nabla_t L(\boldsymbol{\omega}_o, t) &= \nabla \int_\Omega f_r(\boldsymbol{\omega}_{ix}(t), \boldsymbol{\omega}_{ox}(t)) E(\boldsymbol{\omega}'_i)(\mathbf{n}_x(t)\cdot\boldsymbol{\omega}'_i) d\boldsymbol{\omega}'_i \\
&= \nabla_t \int_\Omega \frac{\rho_{dx}}{\pi} E(\boldsymbol{\omega}'_i)(\mathbf{n}_x(t)\cdot\boldsymbol{\omega}'_i) d\boldsymbol{\omega}'_i \\
&\quad + \nabla_t \int_\Omega \rho_{sx} f_{sx}(\boldsymbol{\omega}_{ix}(t), \boldsymbol{\omega}_{ox}(t)) E(\boldsymbol{\omega}'_i)(\mathbf{n}_x(t)\cdot\boldsymbol{\omega}'_i) d\boldsymbol{\omega}'_i \\
&= \frac{\rho_{dx}}{\pi} \nabla_t \int_\Omega E(\boldsymbol{\omega}'_i)(\mathbf{n}_x(t)\cdot\boldsymbol{\omega}'_i) d\boldsymbol{\omega}'_i \\
&\quad + \rho_{sx} \nabla_t \int_\Omega f_{sx}(\boldsymbol{\omega}_{ix}(t), \boldsymbol{\omega}_{ox}(t)) E(R_{nx(t)}(\boldsymbol{\omega}_i)) \boldsymbol{\omega}_{iz} d\boldsymbol{\omega}'_i
\end{aligned} \quad . \quad (6)$$

There are two terms in Eq.6, diffuse reflection component and specular reflection component. Because temporal variation of diffuse component is comparatively small, temporal gradient of the diffuse component can be assumed approximately zero. Hence, specular component, which is principally effected by lighting, is the dominant factor of outgoing radiance denoted as Eq.7.

$$L(\boldsymbol{\omega}'_o, x, t) \approx \rho_s(x) \int_\Omega f_{sx}(\boldsymbol{\omega}_i, \boldsymbol{\omega}_o(t)) \boldsymbol{\omega}_{iz} E(R_{nx(t)}(\boldsymbol{\omega}_i)) d\boldsymbol{\omega}'_i \quad . \quad (7)$$

Taking that approximation, we can simply solve the minimization problem denoted in Eq.8 with temporal gradient of the observation and outgoing radiance denoted in Eq.7.

$$\underset{D'_x}{\arg\min} \sum_t \| \nabla_t T(\boldsymbol{\omega}'_o, t) - \int_\Omega f_{sx}(\boldsymbol{\omega}_i, \boldsymbol{\omega}_o(t)) \boldsymbol{\omega}_{iz} E(R_{nx(t)}(\boldsymbol{\omega}_i)) d\boldsymbol{\omega}' \|^2 \quad , \quad (8)$$

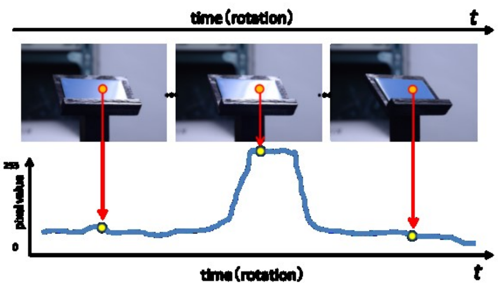

Figure 3

Temporal variation of pixel value during the measurement

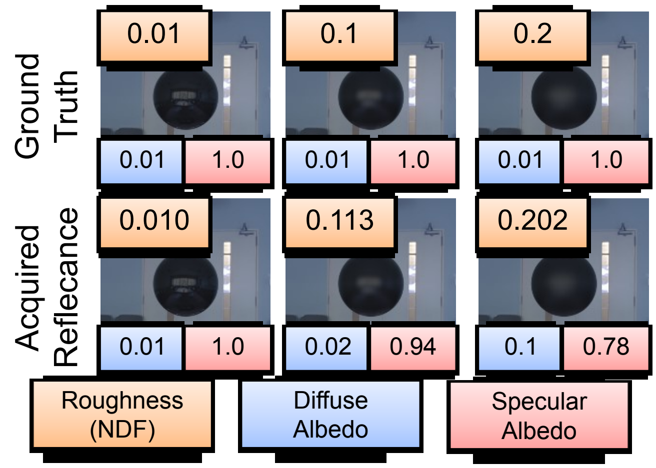

Figure 4

Results of synthetic image generated by Mitsuba renderer with calculated three variables.

where D'_x is the unnormalized NDF biased by specular albedo ρ_{sx}. Finally, the NDF D_x is recovered from D'_x via unit integration.

In our implementation, we employ two NDFs, Beckmann distribution and GGX distribution. It is expected that residual of minimization problem may be reduced if the characteristics of NDF is suitable for representing the surface reflectance of target object. We adopt the result which has smaller residual value for verifying the accuracy of our proposed method.

Albedo Recovery

Given the recovered NDF D_x from previous formulation, we can now determine the diffuse component and specular component of outgoing radiance denoted as Eq.9.

$$\begin{aligned}
T_{dx}(\boldsymbol{\omega}_o, t) &= \int_\Omega f_r(\boldsymbol{\omega}_{ix}(t), \boldsymbol{\omega}_{ox}(t)) E(\boldsymbol{\omega}'_i)(\mathbf{n}_x(t)\cdot\boldsymbol{\omega}'_i) d\boldsymbol{\omega}'_i \\
&= \frac{\rho_{dx}}{\pi} \int_\Omega E(\boldsymbol{\omega}'_i)(\mathbf{n}_x(t)\cdot\boldsymbol{\omega}'_i) d\boldsymbol{\omega}'_i \\
&\quad + \rho_{sx} \int_\Omega f_{sx}(\boldsymbol{\omega}_{ix}, \boldsymbol{\omega}_{ox}) E(\boldsymbol{\omega}'_i)(\mathbf{n}_x(t)\cdot\boldsymbol{\omega}'_i) d\boldsymbol{\omega}'_i \\
&= \rho_{dx} T_{dx}(\boldsymbol{\omega}'_o, t) + \rho_{sx} T_{sx}(\boldsymbol{\omega}'_o, t)
\end{aligned} \quad . \quad (9)$$

$T_{dx}(\boldsymbol{\omega}'_o,t)$ and $T_{sx}(\boldsymbol{\omega}'_o,t)$ are diffuse trace and specular trace of the outgoing radiance. It can be regarded that the observation trace $T(\boldsymbol{\omega}'_o,t)$ is the weighed sum of normalized diffuse trace and specular trace. As a result, recovery of the albedo components are formulated as non-negative least squares minimization problem as shown in Eq.10.

$$\underset{(\rho_d,\rho_s)_x}{\arg\min} \sum_t \| T_x(\boldsymbol{\omega}'_o,t) - (\rho_{dx} T_{dx}(\boldsymbol{\omega}'_o,t) + \rho_{sx} T_{sx}(\boldsymbol{\omega}'_o,t)) \|^2 \ . \quad (10)$$

Verification

In order to validate our proposed method, we prepare synthetic image generated by Mitsuba renderer [22]. We rendered three kinds of objects by changing surface reflectance as shown in upper row of Fig.4. These images rendered with the office window environment map (Fig.1) and used Beckmann distribution, and lower row images were rendered by using the acquired surface reflectance from our proposed method. Comparing upper to lower images, it can be confirmed that the calculated surface reflectance properties can make a reasonable image with our proposed method. Though the calculated parameters of the most right one in upper and lower row are different, visual difference is slightly small.

We also evaluated the validity of our proposed method by comparing with the NDF acquired by gonio-photometer. Figure 5 shows the results of measurement by using gonio-photometer and our proposed method, where blue line in the Fig.5 is measured by gonio-photometer, and red line and green line in Fig.5 are Beckmann distribution model and GGX distribution model, respectively. As we expected, surface reflectance of each target object is recovered by appropriate NDF to represent each material. It is apparent that NDFs of each of the subjects are estimated accurately as same as the gonio-photometer.

Another priority of our proposed method is reduction of computational cost. Since our proposed method uses environmental map as the incident light component, the computational cost is simply reduced. Not to require the estimation of incident light component, we can estimate each surface reflectance independently. Therefore, the parallel computing technique is easy to apply for our proposed method, and it can accelerate estimation process dramatically. We estimate the computational cost of both our proposed and previous method. As the result, our proposed method achieves ten times faster.

Discussion

We measured other 3D objects as shown in Fig.6, in which left side shows real objects and right side shows rendered objects. Here, it is noted that we have no choice but to estimate by the appearance since it is difficult to acquire the ground truth of these 3D object. Despite color matching

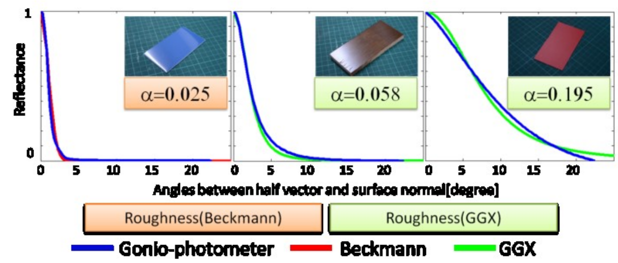

Figure 5

Measurement results of reflectance by using our proposed method and gonio-photometer.

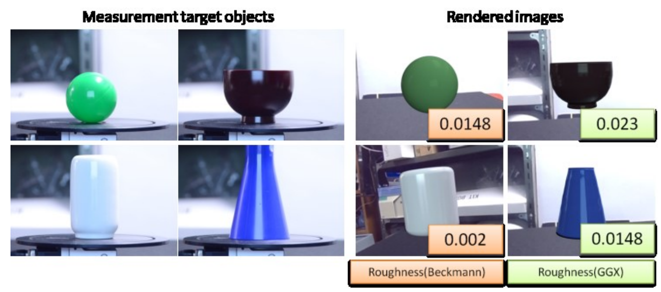

Figure 6

3D real objects and their reproductions derived by our proposed method.

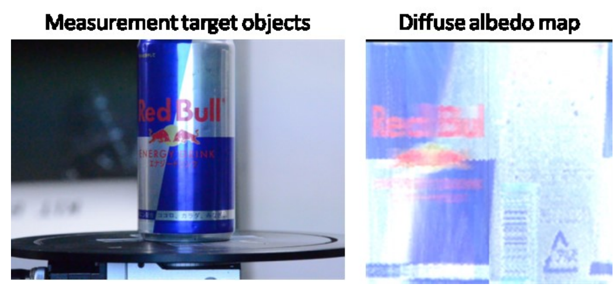

Figure 7

Measurement result of diffuse albedo map of aluminum can with detailed texture.

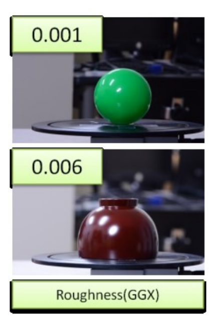

Figure 8

Another measurement which failed to derive the surface reflectance properties.

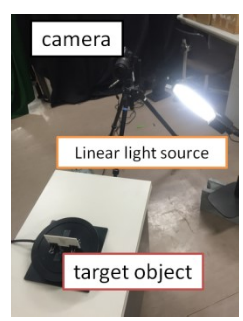

Figure 9

Measurement environment of Fig.8

between real object and reproduction is still not perfect, the appearance of specular highlights resembles in each other.

In order to evaluate the measurement of diffuse texture map, we measured the aluminum cans with texture of surfacing coat as shown in Fig.7. The diffuse albedo map by lining up the measurement result is shown in the right side of Fig.7. From the result, we observe that texture is blurred and detail of texture is lost. It is assumed that this blurriness was caused by lack of surface points on the geometry data. In our implementation, the registered geometry is not so dense and causes the short of vertices. If we have to make the reproduction with complicate texture, highly dense vertex is necessary to calculate and render the detailed reflectance information, even if the calculation cost is increased.

The environmental map captured from omni-directional camera is also effect to the result. Fig 8 shows another measurement result of target object (Fig.6) under different place. In this measurement, the highlight on the target object is not appeared because of positional relation between target object and light source (fluorescent ceiling light). Thus, we set another linear light source next to the camera as shown in Fig.9. Consequently, the result is quite different from first measurement. Sharpness in the BRDF is determined by surface roughness or blurriness of light source. The distance of omni-directional camera and light source causes unexpected measurement error. In this case, we set the linear light source close to the Ricoh Theta. Thus, the light source in captured image is expanded or blurred because of saturation or lens flare. To avoid those measurement error, it is required that we would pay attention for measurement

Conclusion and Future Work

In this paper, we present a simple BRDF measurement method with well-convergence and rapid estimation by adding the lighting component derived from omni-directional camera. Though our method is simplified from previous study, we can demonstrate the superiority of using omni-directional camera. For the reproduction phase, such as three-dimensional printing or computer graphics, color matching problem is important for reproduce the appearance correctly. We measured relatively simple object for verifying the performance of our proposed method. As the results, are we can estimate the surface reflectance accurately as same as the gonio-photometer. Moreover, our proposed method achieves ten times faster owing to the simplification of incident light component.

From the practical point of view, it is necessary to evaluate the target object with more complex shape. The dense of geometry data is also important to acquire detailed result. We need to Although the improvement of omni-directional cameras is remarkable, controlling the saturation or lens flare seems to be difficult because of specialty of fisheye lens. Therefore, image processing which control the appropriate representation of light source in environmental map image is required. Further improvement is necessary, this development would be useful for the widely application of rapid proto-typing.

Acknowledgement

This research was partially supported by the Ministry of Education, Science, Sports, and Culture, Japan Grant-in-Aid for Scientific Research, 24500267, 15K00415, and Brain and Information Science on SITSUKAN, 25135707.

References

[1] Dong, Yue, et al. "Appearance-from-motion: recovering spatially varying surface reflectance under unknown lighting."ACM Transactions on Graphics (TOG)33.6 (2014): 193.

[2] Ryota Domon, et al. " Accelerating computation of Appearance from Motion by using Omni-Directional Camera "Japanese Society of Applied Physics(2016).

[3] Matusik, W., Pfister, H., Brand, M., and McMillan, L., "Efficient Isotropic BRDF Measurement",Proc.Eurographics Symposium on Rendering, pp. 241—247, (2003).

[4] Ezra, M.B., Wang, J., Wilburn, B., Li, X., and Ma, L., "An LED-only BRDF measurement device", IEEE conference on computer vision and pattern recognition, pp. 1-8, (2008).

[5] Gardner, A., Tchou, C., Hawkins, T., and Debevec, P., "Linear Light Source Reflectometry",ACM Transactions on Graphics 22, 3, pp. 749-758, (2003).

[6] Wang, J., Zhao, S., Tong, X., Snyder, J., and Guo, B., "Modeling Anisotropic Surface Reflectance with Example-Based Microfacet Synthesis", ACM Transactions on Graphics,pp. 1-9, (2008).

[7] Ren, P., Wang, J., Snyder, J., Tong, J. X., and Guo, B., "Pocket Reflectometry", ACM Transactions on Graphics 30, 4, pp. 45:1-45:10, (2011).

[8] Alldrin, N., Zickler, T., and Kriegman, D., "Photometric StereoWith Non-Parametric and Spatially-Varying Reflectance", Vision and Pattern Recognition, pp. 1-8, (2008).

[9] Ghosh, A., Chen, T., Peers, P., Wilson, C. A., and Debevec, P., "Circularly Polarized Spherical Illumination Reflectometry", ACM Transactions on Graphics 29, pp. 162:1-162:12, (2010).

[10] Ghosh, A., Fyffe, G., Tunwattanapong, B., Busch, J., Yu X., and Debevec, P., "Multiview Face Capture using Polarized Spherical Gradient Illumination", Eurographics Symposium on Rendering, Proc.SIGGRAPH Asia, pp.129:1-129:10, (2011).

[11] Makino, T., Tsumura, N., Takase, K., Homma, R., Nakaguchi, T., Ojima, N., and Miyake, Y., " Development of the Measurement System for Facial Physical Properties with the 50 Short-Distance Lighting ", Journal of Imaging Science and Technology, 53, 6, pp.605011-605019, (2009).

[12] Hasegawa, T., Tsumura, N., Nakaguchi, T., and Iino, ., "Photometric approach to surface reconstructionof artist paintings", Journal of Electronic Imaging 20(1), 01300, (2011).

[13] Holroyd, M., Lawrence, J., and Zickler, T., "A Coaxial Optical Scanner for Synchronous Acquisition of 3D Geometry and Surface Reflectance", ACM Transactions on Graphics 29, 4, pp. 99:1—99:12, (2010).

[14] Dong, Y., Snyder, J., Tong, X., Snyder, J., Lan, Y., Benezra M., and Guo, B., "ManifoldBootstrapping for SVBRDF Capture", ACM Transactions on Graphics 29, 4, pp. 98:1−98:10, (2010).

[15] Schwartz, C., Weinmann, M., Ruiters, R., Zinke A., and Sarlette, R., "Capturing Shape and Reflectance of Food", SIGGRAPH Asia, 2011 Sketches, p.28.

[16] Naik, N., Zhao, S., Velten, A., Raskar, R., & Bala, K. (2011, December). Single view reflectance capture using multiplexed scattering and time-of-flight imaging. In ACM Transactions on Graphics (TOG) (Vol. 30, No. 6, p. 171). ACM.

[17] Aittala, M., Weyrich, T., and Lehtinen, J., "Practical SVBRDF Capture In The Frequency Domain", ACM Transactions on Graphics 32, 4, (2013).
[18] Christophe Schlick. "An inexpensive BRDF model for physically-based rendering," Computer Graphics Forum, 13(3):233—246, 1994.
[19] Zhang, Zhengyou. "A flexible new technique for camera calibration." Pattern Analysis and Machine Intelligence, IEEE Transactions on 22.11 (2000): 1330-1334.
[20] Debevec, Paul E., and Jitendra Malik. "Recovering high dynamic range radiance maps from photographs." ACM SIGGRAPH 2008 classes. ACM, 2008.
[21] Ashikhmin, Michael, and Peter Shirley. "An anisotropic phong BRDF model."Journal of graphics tools 5.2 (2000): 25-32.
[22] Mitsuba Renderer, "https://www.mitsuba-renderer.org/"